Journal of Associated Medical Sciences 2026; 59(2): 142-152

JAMS
Journal of Associated Medical Sciences

Scopus Indexed & Thai-Journal Citation Index Centre (TCI)

Journal of Associated Medical Sciences

Journal homepage: https://www.tci-thaijo.org/index.php/bulletinAMS/index

Fabrication and evaluation of 3D-printed customizable boluses for optimized radiotherapy applications

Chitchaya Suwanraksa[1], Athitan Khiewded[2], Gadesuda Jankaew[1], Thirawut Rojchanaumpawan[1], Surapong Chatpun[3], Pornchai Phukpattaranont[2*]

[1]*Department of Radiology, Faculty of Medicine, Prince of Songkla University, Songkhla Province, Thailand.*
[2]*Department of Electrical and Biomedical Engineering, Faculty of Engineering, Prince of Songkla University, Songkhla Province, Thailand.*
[3]*Department of Biomedical Sciences and Biomedical Engineering, Faculty of Medicine, Prince of Songkla University, Songkhla Province, Thailand.*

ARTICLE INFO

Article history:
Received 17 November 2025
Accepted as revised 5 February 2026
Available online 9 February 2026

Keywords:
3D printing, radiotherapy, bolus fabrication, polylactic acid.

ABSTRACT

Background: Commercial radiotherapy boluses often fail to conform accurately to patient anatomy, resulting in air gaps and surface dose inaccuracy. Three-dimensional (3D) printing using fused deposition modeling with polylactic acid (PLA) offers a customizable alternative, but clinical implementation requires a reproducible fabrication workflow that ensures both radiological consistency and geometric conformity.

Objectives: To evaluate the effect of infill density on radiological properties and assess the feasibility of a consistent fabrication approach for both standard and patient-specific boluses.

Materials and methods: Standard PLA boluses (10×10×1 cm) were fabricated at 75-95% infill density using a line infill pattern, while customized boluses were created from a head-and-neck phantom and printed at 90-95% infill density. All boluses underwent CT imaging and were analyzed in the Eclipse treatment planning system (TPS) to determine Hounsfield unit (HU), mass density, and relative electron density (RED). Air gap measurements and dose distributions were evaluated in the TPS with a 6 MV photon beam.

Results: As infill density increased from 75%-95%, HU values rose from -184.6 to +48.5, with 90–94% infill yielding HU values within the acceptable ±50 HU range. Standard and customized boluses demonstrated comparable radiological behavior, with mass density and RED near unity. Customized boluses reduced air gaps (0.21±0.02 cm vs 0.54±0.16 cm) and improved surface-dose build-up and isodose coverage in complex regions.

Conclusion: Optimized infill density settings support a reproducible 3D printing workflow. Both standard and customized PLA boluses can achieve radiological accuracy and surface conformity suitable for clinical implementation.

***Corresponding contributor.**
Author's Address: *Department of Electrical and Biomedical Engineering, Faculty of Engineering, Prince of Songkla University, Songkhla Province, Thailand.*
E-mail address: pornchai.p@psu.ac.th
doi: 10.12982/JAMS.2026.046
E-ISSN: 2539-6056

Introduction

Radiotherapy is a fundamental treatment for malignant and non-malignant tumors that utilizes high-energy ionizing radiation to eliminate cancer cells and inhibit tumor growth.[1] Recently, modern radiotherapy techniques have advanced to maximize tumor control while minimizing damage to surrounding healthy tissues.[2] Linear accelerators generate megavoltage photon beams that have the characteristic of delivering peak radiation doses deposited below the skin at

the depth of the maximum dose (Dmax), called a skin-sparing effect.[3] While this characteristic is advantageous for treating deep-seated tumors, it poses challenges for delivering precise surface doses for superficial tumors, including skin cancers, post-mastectomy chest wall recurrences, and superficial lymph node involvement. Achieving adequate dose coverage for these superficial lesions remains a significant challenge.[4,5] To overcome this limitation, a bolus, which is a tissue-equivalent material, is applied to the patient's skin to increase the surface dose by shifting the Dmax toward the skin surface.[6-8] Commercial boluses are mass-produced and lack the flexibility to provide patient-specific design options. They often fail to conform to complex body contours, leading to air gaps between the bolus and the skin surface. These air gaps result in dose inhomogeneity and compromise the accuracy of surface dose delivery.[9,10] In some cases, commercial boluses are manually cut or modified to fit specific patient anatomies, which can lead to material waste and still fail to achieve the desired level of precision.[11] In addition, manual fabrication increases preparation time and operator workload, adding to overall treatment costs and reducing clinical throughput in busy radiotherapy departments. These limitations highlight the need for a fabrication method that is both geometrically accurate and operationally efficient.

In treatment planning, the radiological properties of bolus materials expressed by Hounsfield unit (HU), mass density, and relative electron density (RED) directly influence dose calculation accuracy. Therefore, maintaining consistent HU/RED characteristics between the planned and delivered setup is essential for reliable surface-dose estimation and quality assurance.[12]

While commercial boluses are suitable for routine treatments, advances in additive manufacturing have introduced opportunities to improve workflow efficiency, reproducibility, and customization through patient-specific design. Three-dimensional (3D) printing enables the fabrication of boluses that closely match individual anatomy and maintain stable radiological properties.[13]

Among various additive manufacturing techniques, fused deposition modeling (FDM) has emerged as a particularly promising method for producing patient-specific boluses, constructing physical objects directly from digital models by layering extruded thermoplastic materials.[14] Polylactic acid (PLA) is a thermoplastic widely used in medical applications, including radiotherapy bolus fabrication. Its excellent printability enables the precise and stable production of complex shapes. PLA's mechanical strength preserves structural integrity during repeated treatments, and its radiological properties can be adjusted through infill density to achieve HU values within a clinically acceptable range and with low variability, supporting dose consistency in treatment planning.[15] The adaptability of PLA facilitates the creation of 3D-printed boluses that support accurate surface dose delivery during radiotherapy as planned in treatment simulations.[16–18] The combination of FDM printing technology and PLA material provides a cost-effective, customizable, and scalable solution for producing high-precision, patient-specific boluses. The use of a commercially available 3D printer demonstrates strong potential for translating this methodology into routine clinical workflows, offering a practical solution to both technical and economic challenges in bolus production.[19] Despite significant advancements in 3D-printed boluses for radiotherapy, critical gaps remain in their clinical adoption. Although recent studies have examined HU accuracy, dose distribution, and air-gap reduction,[20-22] a streamlined and systematic evaluation of design, fabrication, and integration processes is still lacking. Key challenges include ensuring material integrity, dose uniformity, geometric conformity, and consistency during the transition from standard to patient-specific bolus shapes.

To address these gaps, this study systematically evaluated how infill density in FDM-printed boluses affects key radiological parameters (HU, RED, and mass density) and physical characteristics (surface conformity and geometric consistency), to develop a reproducible fabrication workflow for clinical use. By benchmarking against virtual and commercial boluses, this research aims to provide a robust foundation for the clinical implementation of 3D-printed bolus technology.

Materials and methods

Figure 1 illustrates the methodology employed in this study, comprising two stages: A) fabrication of standard and customized boluses using 3D printing, and B) performance evaluation of the fabricated boluses.

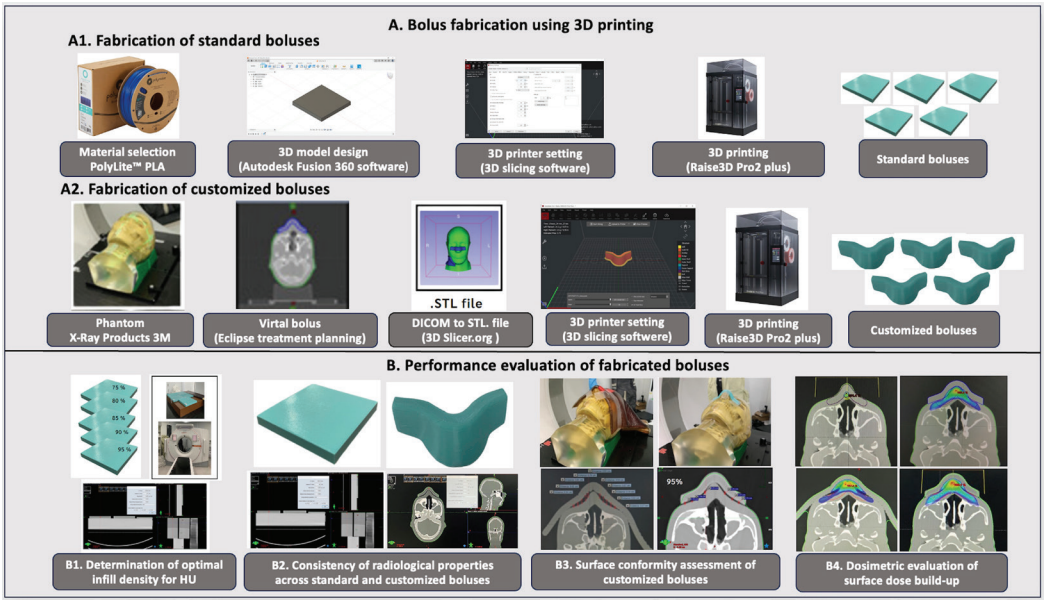

Figure 1. *Schematic representation of the fabrication and evaluation process for 3D-printed customizable boluses, developed to optimize radiotherapy applications.*

3D printing bolus fabrication

Two types of boluses were fabricated for this study: standard and customized. We used the standard bolus as a reference to evaluate the impact of varying infill densities on radiological properties and dosimetric performance. In contrast, the customized bolus was designed to conform to patient-specific anatomical contours, aiming to enhance surface conformity and reduce air gaps. The fabrication procedures for both bolus types are described in detail below.

Fabrication of standard boluses

Standard boluses were digitally designed as rectangular plates measuring 10×10×1 cm using 3D design software (Fusion 360; Autodesk Inc., San Rafael, CA, USA). The 3D model of the rectangular plate was exported as an STL file, which was used as an input for 3D printing. Boluses were fabricated via FDM using a Raise3D Pro2 Plus 3D printer (Raise3D Technologies, Irvine, CA, USA). The PLA filament (PolyLite™ PLA; Polymaker, Shanghai, China) was selected for its high stiffness and tensile strength, radiological equivalence, and ease of handling during printing.[23] The filament, with a diameter of 1.75 mm and density of 1.19 gm/cm^3, enabled consistent extrusion and dimensional stability, which are critical for ensuring the quality and accuracy of the printed boluses. The slicing parameters were configured using a 3D slicing software (IdeaMaker, Raise3D Technologies, Irvine, CA, USA), with settings adjusted to balance print quality and fabrication efficiency while minimizing structural defects. Key parameters, including layer height, print speed, extruder temperature, and infill pattern, were carefully selected to ensure precision and reproducibility. The printing parameters are summarized in Table 1.

Table 1. Printing parameters configured using 3D slicing software.

Printing parameters	Values
Layer height	0.2 mm
Number of shells	2
Nozzle diameter	0.4 mm
Nozzle temperature	230 °C
Bed temperature	60 °C
Printing speed	120 mm/s
Infill pattern	Line

A total of five boluses were fabricated for each infill density (75%, 80%, 85%, 90%, 95%) to evaluate measurement reproducibility. All boluses were printed and stored under controlled environmental conditions to minimize the moisture sensitivity of PLA before CT imaging. Each HU and RED measurement was repeated three times on separate CT acquisitions to confirm consistency.

To systematically investigate the effect of infill density on radiological properties, standard boluses were printed with infill densities incrementally adjusted in 5% steps: 75%, 80%, 85%, 90%, and 95%. Additional boluses were fabricated for precise tuning with density adjustments in 1% steps within the range closely approximating water equivalence (0 HU). Each fabricated bolus was visually inspected for structural integrity, dimensional accuracy, and surface uniformity before being subjected to further testing. This procedure ensured that only boluses meeting quality standards were included in subsequent evaluations.

Fabrication of customized boluses

Customized boluses were designed to replicate patient-specific anatomical contours to improve surface conformity and minimize air gaps. An anthropomorphic head-and-neck phantom manufactured by the X-Ray Products Division of 3M (USA) was scanned using a Siemens SOMATOM GoPro CT Scanner (Siemens Healthineers, Erlangen, Germany) at 120 kVp with a slice thickness of 1 mm for accurate imaging. CT images were imported into the Eclipse treatment planning system (TPS) (Version 16.0, Varian Medical Systems, Palo Alto, CA, USA) to generate a virtual bolus with HU of 0, mass density of 1.0081 gm/cm^3, RED of 1.0061, and uniform thickness of 1 cm. The DICOM file of the virtual bolus was converted to an STL file using 3D Slicer (3D Slicer.org, Boston, Massachusetts, USA) to ensure compatibility with the 3D printing workflow.

The customized boluses were fabricated using the same 3D printing process as that for the standard boluses. The printing parameters listed in Table 1 were applied to ensure consistency in fabrication quality. Infill densities were varied between 90% and 95% in 1% steps to evaluate performance. Following fabrication, the customized boluses were inspected for dimensional accuracy, structural integrity, and surface conformity. Alignment with the phantom's anatomical contours was verified to ensure their suitability for radiotherapy applications. Figure 2 shows examples of the 3D-printed standard and customized boluses.

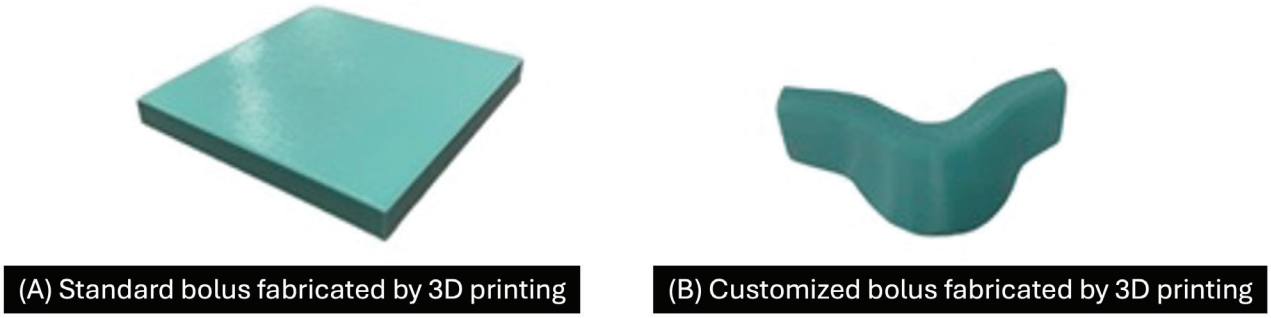

Figure 2. Examples of 3D-printed bolus fabrication in this study. (A) standard bolus, and (B) customized bolus.

Performance evaluation of fabricated boluses

The performance of the fabricated boluses was systematically analyzed through four evaluations, focusing on radiological properties, surface conformity, and dosimetric accuracy, to ensure that the fabricated boluses meet the requirements for radiotherapy applications.

Determination of optimal infill density for HU

This evaluation aimed to determine the infill density that yielded a HU value within a clinically acceptable range close to 0, representing radiological behavior consistent with that assumed in treatment planning. Standard boluses with infill densities of 75%, 80%, 85%, 90%, and 95% were each fabricated in triplicate and CT-scanned using a Siemens SOMATOM GoPro scanner at 120 kVp, 200 mA, 1-mm slice thickness, and a 250-mm field of view. The boluses were stored at room temperature before CT imaging. HU values were measured from a centrally placed region of interest on the mid-plane of each bolus and averaged across three consecutive slices to minimize local variation. The mean±SD of HU, mass density, and RED were determined for each infill density to assess measurement reproducibility.

Consistency of radiological properties across standard and customized boluses

After identifying the infill densities that yielded HU values within a clinically acceptable range close to 0, both standard and customized boluses were fabricated using identical infill densities to ensure comparable material characteristics irrespective of geometry. Each bolus was CT-scanned to determine HU, mass density, and RED values. The measured parameters were compared to assess the consistency of radiological properties between the two bolus designs.

Surface conformity assessment of customized boluses

This evaluation aimed to assess surface conformity and air-gap reduction of customized boluses applied to a head-and-neck phantom. Customized boluses with optimized infill densities were fitted onto the phantom and CT-scanned. For comparison, a commercially available bolus commonly used in clinical practice was positioned at the same location on the phantom and scanned under identical imaging conditions. Air gaps between each bolus and the phantom surface were quantified using the Eclipse TPS. The air-gap distance was defined as the perpendicular separation between the outer contour of the phantom and the inner surface of the bolus, identified in axial CT images where discontinuities were observed. The maximum and mean gap distances were measured across the contact region and compared between the customized and commercial boluses to evaluate surface conformity and setup reproducibility.

Dosimetric evaluation of surface dose build-up

The dose distributions of customized boluses were compared with those of three alternatives no bolus, virtual bolus, and a commercially available clinical bolus to evaluate their impact on surface-dose build-up. Treatment planning was performed in the Eclipse treatment planning system (Version 16.0, Varian Medical Systems) using the Anisotropic Analytical Algorithm (AAA) with a 6 MV photon beam generated by a TrueBeam linear accelerator. A single anterior photon field was applied, with the field size adjusted to cover the entire bolus area at a source-to-surface distance (SSD) of 100 cm, simulating a typical setup for superficial irradiation. Dose distributions were analyzed qualitatively using the color-wash display at the 100% isodose level to compare surface coverage under different bolus conditions. The analysis focused on the positional shift of the 100% isodose line toward the phantom surface and the uniformity of coverage across regions with complex geometry. Observations from the Eclipse TPS were used to compare dose build-up and conformity among the no-bolus, virtual-bolus, commercial-bolus, and 3D-printed-bolus configurations.

Results

Determination of optimal infill density for HU

Standard boluses with infill densities ranging from 75% to 95% were evaluated for HU, mass density, and RED values using the TPS. The detailed results presented in Table 2 indicated that boluses with infill densities between 90% and 95% exhibited HU values approaching 0, falling within the clinically acceptable water-like range relative to the virtual bolus used in treatment planning. Based on these findings, additional boluses were fabricated with 1% increments within the 90-95% range to refine the high-infill configuration and verify the consistency of radiological properties near water equivalence. As infill density increased, HU values progressively shifted from negative to positive, reflecting increased material density and X-ray attenuation. HU values close to those of water (≈0 HU) were observed at higher infill densities, accompanied by increases in mass density and RED. The boluses produced at higher infill levels exhibited mean mass density and RED values close to unity, supporting their approximation to water-equivalent behavior. These findings indicate that high-infill configurations fall within the clinically acceptable range for water-equivalent bolus fabrication, suggesting their suitability for accurate dose calculation in radiotherapy applications. In contrast, lower infill densities (<90%) produced substantially lower HU values, indicating under-density and reduced reliability in dose modeling. Therefore, high-infill 3D-printed boluses are recommended to achieve clinically acceptable HU conformity and radiological consistency.

Table 2. HU, mass density (MD), and RED values for 3D-printed standard boluses with varying infill densities (IDs) in percent.

ID (%)	HU	MD (gm/cm^3)	RED
75	–184.63±8.23	0.82±0.008	0.81±0.008
80	–156.83±6.57	0.87±0.012	0.85±0.008
85	–107.50±9.59	0.92±0.011	0.91±0.009
90	–43.83±6.09	0.98±0.005	0.97±0.004
91	–31.33±2.56	0.99±0.006	0.97±0.007
92	–19.67±3.68	0.99±0.001	0.98±0.002
93	–1.17±4.81	1.00±0.003	0.99±0.004
94	13.00±3.00	1.01±0.004	1.01±0.003
95	48.50±8.92	1.06±0.010	1.04±0.007

Consistency of radiological properties across standard and customized boluses

To ensure consistent material properties despite geometric variations, customized boluses were fabricated with 90–95% infill in 1% increments. A head-to-head comparison with the standard design showed a mean HU increase of approximately 21 HU, along with average rises of 0.02 gm/cm^3 in mass density and 0.02 in RED (Table 3). The clinically acceptable HU range was defined as ±50 HU around water (0 HU). Within this high-infill band, HU values entered the acceptable range at the lower end and increased further with higher infill, occasionally exceeding the range. Despite minor differences, the overall HU, density, and RED trends between the standard and customized boluses were consistent, indicating stable radiological behavior across geometries. Corresponding increases in mass density and RED approached unity, supporting water-equivalent behavior at higher infill rates, whereas sub-90% infill produced clearly under-dense, sub-water HU values.

Table 3. HU, mass density (MD), and RED values for 3D-printed customized boluses with varying infill densities (IDs) in percent.

ID (%)	HU	MD (gm/cm^3)	RED
90	–38.00±13.32	0.98±0.009	0.97±0.009
91	–23.70±6.38	0.99±0.003	0.98±0.004
92	17.80±11.39	1.02±0.011	1.01±0.010
93	33.55±10.00	1.04±0.013	1.03±0.009
94	44.00±11.55	1.05±0.014	1.04±0.010
95	60.00±8.78	1.07±0.006	1.05±0.005

Surface conformity assessment of customized boluses

Air gaps between the bolus and phantom were analyzed in the TPS to evaluate surface conformity and the effectiveness of reducing air gaps. Figure 3 shows representative measurements comparing commercial and 3D-printed customized boluses. The 3D-printed boluses demonstrated improved conformity to the phantom surface compared with commercial boluses. The mean air-gap distance for 3D-printed customized boluses was 0.21±0.02 cm (range: 0.19-0.25 cm), which was smaller than that of commercial boluses, 0.54±0.16 cm (range: 0.27-0.76 cm). These results confirm the enhanced surface conformity and effective air-gap minimization achieved with 3D-printed customized boluses.

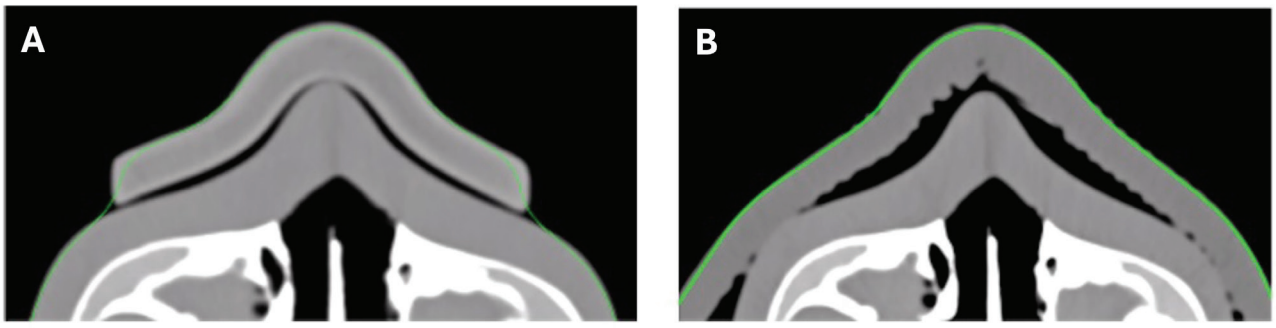

Figure 3. *Comparison of air-gap measurements between the (A) 3D-printed customized bolus and (B) commercial bolus.*

Dosimetric evaluation of surface dose build-up

This analysis evaluated surface dose build-up under different bolus configurations using a 6 MV photon beam in an AP field, as shown in Figure 4. The 100% isodose distribution (yellow region) was assessed under four conditions: no bolus, virtual bolus, commercial bolus, and 3D-printed bolus. Without a bolus, the 100 % isodose line extended deeper into the tissue, demonstrating insufficient surface dose due to the skin-sparing effect of megavoltage photons. The virtual bolus shifted the isodose line toward the surface, simulating an idealized treatment-planning scenario. The commercial bolus improved surface dose uniformity, however, air gaps limited full 100 % isodose coverage, particularly in regions with complex geometry, resulting in potential underdosage. In contrast, the 3D-printed bolus effectively enhanced surface-dose build-up and minimized air gaps. Its customized design provided superior conformity to irregular contours, optimizing dose distribution across the treatment area. Isodose analysis confirmed that the 3D-printed bolus achieved the most complete surface-dose coverage, particularly in complex geometries. These findings demonstrate the feasibility of 3D-printed boluses as customizable alternatives to commercial products, offering enhanced dose conformity and treatment precision.

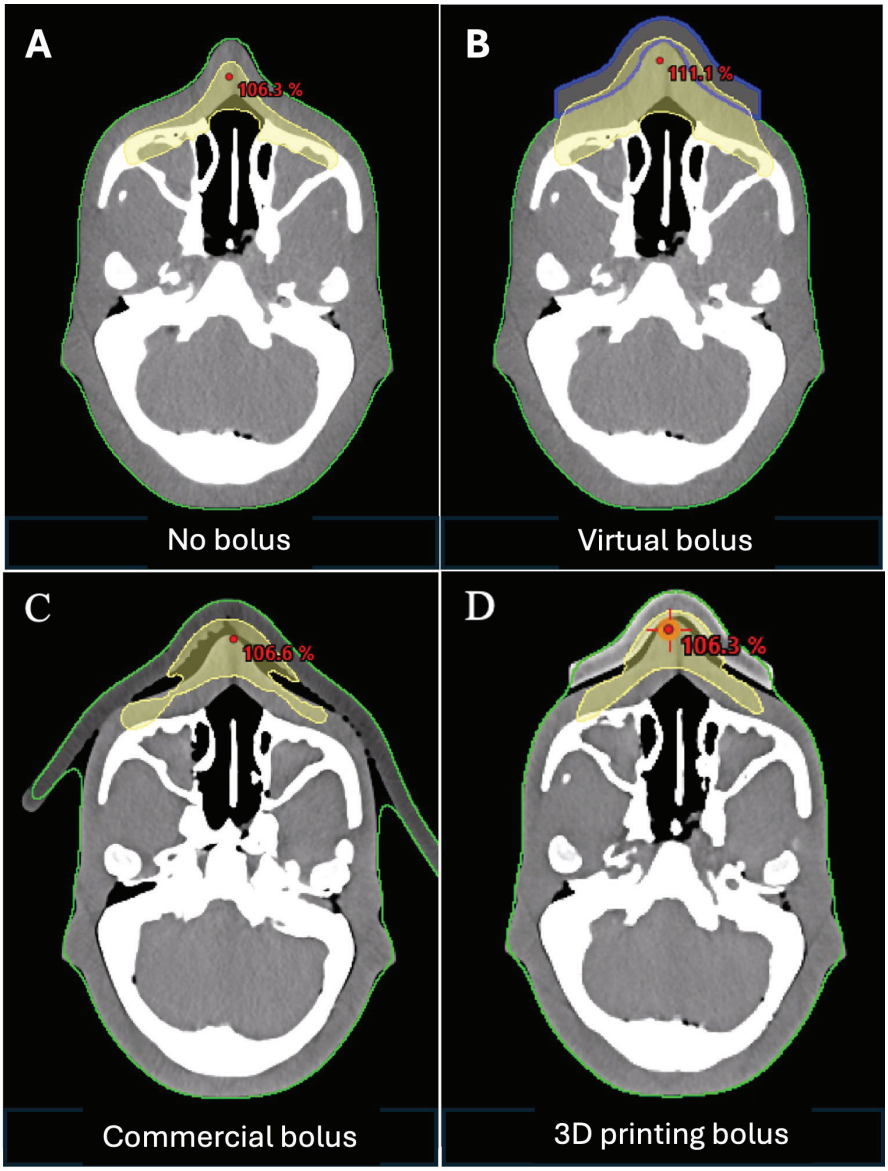

Figure 4. *Comparison of 100% isodose distributions for different bolus configurations using a 6 MV photon beam in an anterior–posterior field. A: without bolus, B: virtual bolus, C: commercial bolus, D: 3D-printed bolus.*

Discussion

This study demonstrated that 3D-printed boluses, when fabricated with optimized infill density, achieved radiological properties within the clinically acceptable water-equivalent range and improved surface conformity compared with commercial boluses. The fabrication process also showed high reproducibility and geometric precision, consistent with previous studies using FDM for radiotherapy applications.[14,15] Fabricating standardized and patient-specific boluses offers enhanced flexibility in treatment planning and reduces inter-operator variability commonly encountered in conventional manual bolus shaping.[24] Our findings confirmed a strong positive correlation between infill density and CT HU, with HU values shifting progressively from negative to positive as infill density increased. In radiotherapy, water-equivalent materials, characterized by HU values near 0, RED≈1.00, and by physical density ≈1.00 g/cm^3, are considered the standard reference for dose calculation in TPS.[8] This standard also reflects common clinical practice, where virtual boluses are typically assigned a HU of 0 during plan optimization. Aligning the HU of physical boluses with this value ensures dosimetric consistency between the planned and delivered dose distributions.[25]

In this study, both standard and customized bolus designs demonstrated similar HU-infill dependence, achieving water-like radiological behavior when printed with dense infill settings. Across the 90-94% infill range, the HU distribution remained within a practical water-equivalent interval (approximately -50 to +50 HU), consistent with prior reports on radiologically water-like 3D-printed bolus materials used in radiotherapy applications.[26,27] In contrast, infill levels below 90% yielded markedly lower HU values, indicating reduced material density and attenuation. Minor HU differences between customized and standard boluses likely reflect geometry-related differences in material deposition rather than true radiological deviations.[18,28,29] These findings suggest that using a dense-infill configuration can ensure radiological consistency across bolus designs, although optimal settings may vary with printer model, filament composition, and infill pattern.

Many studies have employed various approaches to assess the radiological equivalence of 3D-printed boluses. Some targeted HU values near 0 to emulate water-like density,[30] whereas others referenced conventional bolus materials such as Superflab or paraffin wax (approximately -30 to -100 HU) that still achieve RED≈1.00.[31] In addition to HU-based evaluation, several studies have validated dosimetric performance experimentally under photon and electron beams.[18,32] In contrast, the present study relied solely on TPS-based photon dose calculations, with interpretation restricted to the build-up region. No direct physical surface-dose measurements were performed. In addition, uncertainties associated with TPS modeling in this region may therefore influence absolute surface-dose estimation. This reliance on TPS calculations represents a key limitation of the current work. Future work will address this limitation through direct surface-dose measurements using radiochromic film, complemented by parallel-plate ionization chambers for absolute dose verification in the build-up region. In addition, electron-beam dosimetric evaluation will be incorporated to provide more comprehensive clinical validation across beam modalities. The correlation observed between HU and radiological density in this study aligns with previous findings in FDM-printed materials.[17,33] However, acceptable HU tolerances vary across TPS algorithms and clinical settings,[34,35] highlighting the value of density-based QA criteria. For example, Kairn *et al.*[12] proposed ±5% deviation from water-equivalent density as clinically acceptable and ±10 % as an action threshold, providing a practical framework for in-house QA of patient-specific boluses. Customized boluses significantly reduced air gaps compared with commercial boluses. Although bolus placement beneath thermoplastic masks can improve conformity in head-and-neck treatments, this method remains operator-dependent and potentially variable between fractions.

In this study, CT-derived air gap measurements provided a practical quantitative assessment of bolus–skin conformity. Other quantitative air gap measurement methods, such as CT-based HU profile analysis and volumetric air gap quantification using image segmentation, have been reported to provide more detailed geometric characterization of the bolus–skin interface, particularly in regions with complex surface geometry.[36,37] Fixed-geometry 3D-printed boluses may therefore improve reproducibility, setup efficiency, and patient comfort—especially in regions with complex topology, aligning with reports of improved surface-dose build-up with customized bolus fabrication.[38] Isodose analysis further demonstrated improved surface coverage with 3D-printed boluses, supporting their integration into photon-based workflows.[39,40] While electron beams remain standard for very superficial lesions, contemporary photon techniques such as VMAT increasingly rely on bolus for chest-wall and nodal treatments; therefore, photon-based assessment is clinically relevant. Additionally, our results support previous reports that 3D printing offers a potentially cost-efficient alternative to commercial boluses, primarily through reduced material consumption and in-house fabrication.[31] Although the degree of savings depends on local workflows and resources, the ability to individualize bolus design without substantial added expense enhances the scalability of this approach in clinical practice. Material usage (103.5-120.5 gm per standard bolus) and printing time (~4 hours) from this study demonstrate predictable manufacturing demands consistent with prior workflows.[41,42] This supports the practical feasibility of routine clinical deployment.

Limitations

This study used PLA as the primary material for 3D-printed bolus fabrication, which was selected based on a balance of radiological equivalence, mechanical performance, and manufacturing efficiency. While PLA offers advantages such as low ultrafine particle emissions compared with ABS and avoids the release of potentially hazardous thermal decomposition byproducts, alternative materials may provide distinct benefits depending on clinical priorities.[43] For example, silicone-based polymers processed via direct ink writing offer improved flexibility and tissue conformity, but their slow build speeds and limited spatial resolution constrain routine clinical use.[16] Additionally, previous comparative studies have shown that although PLA demonstrates favorable radiation transmission characteristics, materials such as PETG may provide superior mechanical strength and flexibility.[15] Accordingly, future work will systematically evaluate a broader range of printable materials to better balance radiological equivalence, mechanical performance, and manufacturing efficiency.

Another limitation of this study is the use of only one FDM printer model and a specific PLA filament. Variations in printer hardware, such as nozzle calibration, extrusion control, and thermal stability, as well as differences in filament composition and additives across manufacturers, may influence effective infill density and measured HU values. As a result, while the optimal infill density provides a useful benchmark, the reported HU values are specific to the printer–material combination used. Future studies will aim to improve generalizability through validation across multiple FDM systems and filament brands, including multi-center investigations using identical STL geometries. Reporting measured mass and volume to derive physical density, rather than relying solely on slicer-defined infill percentages, may also provide a more universal and reproducible metric.

Finally, this study evaluated only a line infill pattern. However, infill geometry is known to influence internal density distribution, mechanical properties, and manufacturing time. Prior work comparing triangle, honeycomb, honeycomb-gyroid, and gyroid infill patterns in PLA has demonstrated differences in both ultimate tensile strength and HU values.[15] Future investigations will explore diverse infill geometries to identify optimal pattern–density combinations that balance internal density distribution, mechanical properties, and manufacturing time, particularly for boluses with complex anatomical shapes.

Conclusion

This study demonstrated that PLA 3D-printed boluses fabricated with an infill density above 90% achieved radiological properties within the clinically acceptable range for water-like materials and provided superior surface conformity relative to commercial boluses. The fabrication process was highly reproducible, cost-efficient, and suitable for routine in-house clinical implementation. These findings indicate that high-infill 3D-printed boluses can serve as reliable, customizable alternatives to conventional boluses, supporting improved workflow consistency, surface-dose accuracy, and patient comfort in modern radiotherapy practice.

Ethical approval

Ethical approval: REC 68-230-7-2

Funding

This research did not receive any specific grant from funding agencies in the public, commercial, or not-for-profit sectors.

Conflict of interest

The authors declare no conflict of interest for this publication.

CRediT authorship contribution statement

Chitchaya Suwanraksa: conceptualization, methodology, investigation, data collection and analysis, writing: original draft, supervision; **Athitan Khiewded**: methodology, investigation, data collection, and analysis. **Gadesuda Jankaew**: investigation, data collection, and analysis; **Thirawut Rojchanaumpawan**: methodology, data collection, and analysis; **Surapong Chatpun**: methodology, data collection, and analysis. **Pornchai Phukpattaranont**: conceptualization, methodology, investigation, data collection and analysis, writing: original draft, supervision. All authors contributed to reviewing and editing the manuscript and approved the final version for submission.

Acknowledgements

The authors would like to acknowledge the Radiation Oncology Unit, Faculty of Medicine, Prince of Songkla University, for their support and technical assistance throughout this study.

References

[1] Bernier J, Hall EJ, Giaccia A. Radiation oncology: a century of achievements. Nat Rev Cancer. 2004; 4: 737-47. doi:10.1038/nrc1451.

[2] Garibaldi C, Jereczek-Fossa BA, Marvaso G, Dicuonzo S, Rojas DP, Cattani F, et al. Recent advances in radiation oncology. Ecancermedicalscience. 2017; 11: 785. doi:10.3332/ecancer.2017.785.

[3] Khan FM, Gibbons JP Jr. Khan's. The physics of radiation therapy. Philadelphia: Lippincott Williams & Wilkins; 2014: pp 584.

[4] Dogan N, Glasgow GP. Surface and build-up region dosimetry for obliquely incident intensity modulated radiotherapy 6 MV X-rays. Med Phys. 2003; 30: 3091-6. doi:10.1118/1.1625116.

[5] Turner JY, Zeniou A, Williams A, Jyothirmayi R. Technique and outcome of post-mastectomy adjuvant chest wall radiotherapy—the role of tissue-equivalent bolus in reducing risk of local recurrence.

Br J Radiol. 2016; 89(1064): 20160060. doi:10.1259/bjr.20160060.

[6] Hsu SH, Roberson PL, Chen Y, Marsh RB, Pierce LJ, Moran JM. Assessment of skin dose for breast chest wall radiotherapy as a function of bolus material. Phys Med Biol. 2008; 53: 2593-606. doi:10.1088/0031-9155/53/10/010.

[7] Healy E, Anderson S, Cui J, Beckett L, Chen AM, Perks J, et al. Skin dose effects of postmastectomy chest wall radiation therapy using brass mesh as an alternative to tissue-equivalent bolus. Pract Radiat Oncol. 2013; 3: e45-e53. doi:10.1016/j.prro.2012.05.009.

[8] Vyas V, Palmer L, Mudge R, Jiang R, Fleck A, Schaly B, et al. On bolus for megavoltage photon and electron radiation therapy. Med Dosim. 2013; 38: 268-73. doi:10.1016/j.meddos.2013.02.007.

[9] McCallum S, Maresse S, Fearns P. Evaluating 3D-printed bolus compared to conventional bolus types used in external beam radiation therapy. Curr Med Imaging Rev. 2021; 17: 820-31. doi:10.2174/1573405617666210202114336.

[10] Pollmann S, Toussaint A, Flentje M, Wegener S, Lewitzki V. Dosimetric evaluation of commercially available flat vs. self-produced 3D-conformal silicone boluses for the head and neck region. Front Oncol. 2022; 12: 881439. doi:10.3389/fonc.2022.881439.

[11] Davis TM, Luca K, Sudmeier LJ, Buchwald ZS, Khan MK, Yang X, et al. Total scalp irradiation: A study comparing multiple types of bolus and VMAT optimization techniques. J Appl Clin Med Phys. 2024; 25: e14260. doi:10.1002/acm2.14260.

[12] Kairn T, Talkhani S, Charles PH, Chua B, Lin CY, Livingstone AG, et al. Determining tolerance levels for quality assurance of 3D printed bolus for modulated arc radiotherapy of the nose. Phys Eng Sci Med. 2021; 44: 1187-99. doi:10.1007/s13246-021-01054-7.

[13] Fujimoto K, Shiinoki T, Yuasa Y, Hanazawa H, Shibuya K. Efficacy of patient-specific bolus created using three-dimensional printing technique in photon radiotherapy. Phys Med. 2017; 38: 1-9. doi:10.1016/j.ejmp.2017.04.023.

[14] Pugh R, Lloyd K, Collins M, Duxbury A. The use of 3D printing within radiation therapy to improve bolus conformity: a literature review. J Radiother Pract. 2017; 16: 319-25. doi:10.1017/S146039 691 7000115.

[15] Phantawong K, Singthuan N, Pinichsai K, Taertulakarn S. The feasibility of fabricated 3D-printed immobilization masks for radiotherapy: mechanical and dosimetric analysis. J Assoc Med Sci. 2025; 58(3): 361-75.

[16] Lu Y, Song J, Yao X, An M, Shi Q, Huang X. 3D printing polymer-based bolus used for radiotherapy. Int J Bioprint. 2021; 7: 414. doi:10.18063/ijb.v7i4.414.

[17] Van Der Walt M, Crabtree T, Albantow C. PLA as a suitable 3D printing thermoplastic for use in external beam radiotherapy. Australas Phys Eng Sci Med. 2019; 42: 1165-76. doi:10.1007/s13246-019-00818-6.

[18] Ricotti R, Ciardo D, Pansini F, Bazani A, Comi S, Spoto R, et al. Dosimetric characterization of 3D-printed bolus at different infill percentage for external photon beam radiotherapy. Phys Med. 2017; 39: 25-32. doi:10.1016/j.ejmp.2017.06.004.

[19] Ashenafi M, Jeong S, Wancura JN, Gou L, Webster MJ, Zheng D. A quick guide on implementing

[20] and quality assuring 3D printing in radiation oncology. J Appl Clin Med Phys. 2023; 24: e14102. doi:10.1002/acm2.14102.

[21] Şahin T, Çavdar Karaçam S, Tunçman D, Şahin Ş, Ergen ŞA, Çolpan Öksüz D, et al. Thermal, dosimetric and thermo-mechanical characterization of ABS and PLA polymer materials via plastic injection molding for innovative bolus materials in radiotherapy applications. Radiat Phys Chem. 2024; 223: 111901. doi:10.1007/s42247-024-00706-0.

[22] Jreije A, Keshelava L, Ilickas M, Laurikaitiene J, Urbonavicius BG, Adliene D. Development of patient-specific conformal 3D-printed devices for dose verification in radiotherapy. Appl Sci. 2021; 11: 8657. doi:10.3390/app11188657.

[23] Ciobanu AC, Petcu LC, Járai-Szabó F, Bálint Z. Exploring the impact of filament density on the responsiveness of 3D-printed bolus materials for high-energy photon radiotherapy. Phys Med. 2024; 127: 104849. doi:10.1016/j.ejmp.2024.104849.

[24] 3DTechSupplies. PolyLite™ PLA. Available from: http://www.3dtechsupplies.com.au/Products/PolyMaker/PolyLite-PLA. Accessed 6 Jan 2026.

[25] Canters RA, Lips IM, Wendling M, Kusters M, Van Zeeland M, Gerritsen RM, et al. Clinical implementation of 3D printing in the construction of patient-specific bolus for electron beam radiotherapy for non-melanoma skin cancer. Radiother Oncol. 2016; 121: 148-53. doi:10.1016/j.radonc.2016.07.011.

[26] Olch AJ, Gerig L, Li H, Mihaylov I, Morgan A. Dosimetric effects caused by couch tops and immobilization devices: report of AAPM Task Group 176. Med Phys. 2014; 41(6 Part 1): 061501. doi:10.1118/1.4876299.

[27] Mutic S, Palta JR, Butker EK, Das IJ, Huq MS, Loo LND, et al. Quality assurance for computed-tomography simulators and the computed-tomography-simulation process: Report of the AAPM Radiation Therapy Committee Task Group No. 66. Medical Physics. 2003; 30(10): 2762-92.

[28] Burleson S, Baker J, Hsia AT, Xu Z. Use of 3D printers to create a patient-specific 3D bolus for external beam therapy. J Appl Clin Med Phys. 2015; 16(3): 5247. doi: 10.1120/jacmp.v16i3.5247.

[29] Savi M, Potiens MPA, Cechinel CM, Silveira LC, Soares FAP. Relationship between infill patterns in 3D printing and Hounsfield Unit. In: Proceedings of the International Joint Conference RADIO 2017: Goiania 30 Years Later; 2017 Oct; Goiania, Brazil.

[30] Biltekin F, Yazici G, Ozyigit G. Characterization of 3D-printed bolus produced at different printing parameters. Med Dosim. 2021; 46: 157-63. doi:10.1016/j.meddos.2020.10.005.

[31] Jeong S, Yoon M, Chung WK, Kim DW. Preliminary study of the dosimetric characteristics of 3D-printed materials with megavoltage photons. J Korean Phys Soc. 2015; 67(1): 189-94. doi:10.3938/jkps.67.189.

[32] Albantow C, Hargrave C, Brown A, Halsall C. Comparison of 3D-printed nose bolus to traditional wax bolus for cost-effectiveness, volumetric accuracy and dosimetric effect. J Med Radiat Sci. 2020; 67: 54-63. doi:10.1002/jmrs.378.

[33] Kim SW, Shin HJ, Kay CS, Son SH. A customized bolus produced using a 3-dimensional printer for radiotherapy. PLoS One. 2014; 9: e110746. doi:10.1371/journal.pone.0110746.

[34] Dancewicz OL, Sylvander SR, Markwell TS, Crowe SB, Trapp JV. Radiological properties of 3D-printed materials in kilovoltage and megavoltage photon beams. Phys Med. 2017; 38: 111-8. doi:10.1016/j.ejmp.2017.05.051.

[35] Burleson S, Baker J, Hsia AT, Xu Z. Use of 3D printers to create a patient-specific 3D bolus for external beam therapy. J Appl Clin Med Phys. 2015; 16: 166-78. doi:10.1120/jacmp.v16i3.5247.

[36] Park SY, Choi CH, Park JM, Chun M, Han JH, Kim JI. A patient-specific polylactic acid bolus made by a 3D printer for breast cancer radiation therapy. PLoS One. 2016; 11: e0168063. doi:10.1371/journal.pone.0168063.

[37] Dipasquale G, Poirier A, Sprunger Y, Uiterwijk JWE, Miralbell R. Improving 3D-printing of megavoltage X-rays radiotherapy bolus with surface-scanner. Radiat Oncol. 2018; 13(1): 203. doi: 10.1186/s13014-018-1148-1.

[38] Gugliandolo SG, Pillai SP, Rajendran S, Vincini MG, Pepa M, Pansini F, et al. 3D-printed boluses for radiotherapy: influence of geometrical and printing parameters on dosimetric characterization and air gap evaluation. Radiol Phys Technol. 2024; 17(2): 347-59. doi: 10.1007/s12194-024-00782-1.

[39] Łukowiak M, Boehlke M, Lewocki M, Jezierska K, Piatek-Hnat M, Lewocki M, et al. Use of a 3D printer to create a bolus for patients undergoing tele-radiotherapy. Int J Radiat Res. 2016; 14: 287-95. doi:10.18869/acadpub.ijrr.14.4.287.

[40] Łukowiak M, Jezierska K, Boehlke M, Więcko M, Łukowiak A, Podraza W, et al. Utilization of a 3D printer to fabricate boluses used for electron therapy of skin lesions of the eye canthi. J Appl Clin Med Phys. 2017; 18: 76-81. doi:10.1002/acm2.12013.

[41] Sasaki DK, McGeachy P, Alpuche Aviles JE, McCurdy B, Koul R, Dubey A. A modern mold room: Meshing 3D surface scanning, digital design, and 3D printing with bolus fabrication. J Appl Clin Med Phys. 2019; 20: 78-85. doi:10.1002/acm2.12703.

[41] Basaula D, Hay B, Wright M, Hall L, Easdon A, McWiggan P, Yeo A, Ungureanu E, Kron T. Additive manufacturing of patient-specific bolus for radiotherapy: large-scale production and quality assurance. Phys Eng Sci Med. 2024;47:551–61. doi:10.1007/s13246-024-01385-1.

[42] Ehler E, Sterling D, Dusenbery K, Lawrence J. Workload implications for clinic workflow with implementation of three-dimensional printed customized bolus for radiation therapy: a pilot study. PLoS One. 2018;13(10):e0204944. doi:10.1371/journal.pone.0204944.

[43] Stephens B, Azimi P, El Orch Z, Ramos T. Ultrafine particle emissions from desktop 3D printers. Atmos Environ. 2013; 79: 334–339. doi: 10.1016/j.atmosenv.2013.06.050.